Temporal dissociation between local and global functional adaptations of the maternal brain to childbirth: A longitudinal assessment

Leon D. Lotter[1,2,3]*, Susanne Nehls[4,5], Elena Losse[4], Juergen Dukart[1,2], Natalia Chechko[1,4,5]*

[1] Institute of Neuroscience and Medicine, Brain & Behavior (INM-7), Research Centre Jülich; Jülich, Germany.

[2] Institute of Systems Neuroscience, Medical Faculty, Heinrich Heine University Düsseldorf; Düsseldorf, Germany.

[3] Max Planck School of Cognition; Stephanstrasse 1A, Leipzig 04103, Germany.

[4] Department of Psychiatry, Psychotherapy and Psychosomatics, Medical Faculty, RWTH Aachen; Aachen, Germany.

[5] Institute of Neuroscience and Medicine, JARA-Institute Brain Structure Function Relationship (INM-10), Research Centre Jülich; Jülich, Germany.

* Corresponding authors: nchechko@ukaachen.de; l.lotter@fz-juelich.de

Short title: Temporal dissociation between local and global functional adaptations of maternal brain

Display elements:

Table 1

Figures 1–4

Extended Data Tables 1–3

Extended Data Figure 1

Supplementary files:

Supplementary Tables S1–S13 (Excel file)

Code notebook (Jupyter notebook file)

Abstract

The maternal brain undergoes significant reorganization during birth and the postpartum period. However, the temporal dynamics of these changes remain unclear. Using resting-state functional magnetic resonance imaging, we report on local and global brain-functional alterations in 75 mothers in their first postpartum week. In a subsample followed longitudinally for the next 6 months, we observe a temporal and spatial dissociation between baseline changes. Neocortical regions showed persistent local activity and connectivity changes throughout the study, with preliminary evidence linking these alterations to behavioral and psychological adaptations. In contrast, the initially reduced whole-brain connectivity in subcortical areas returned to control levels within 6 to 9 weeks postpartum. Blood hormone association and neuroimaging spatial colocalization analyses suggest that postpartum restoration of progesterone levels may underlay this rapid normalization. These results enhance our understanding of healthy maternal brain function and contribute to identification of potential markers for pathological postpartum adaptation processes.

1. Introduction

The maternal brain experiences major biological and psychological changes during pregnancy and the early postpartum period, suggesting adult brain neuroplasticity. Maternal brain structure of early mothers shows widespread changes in gray matter volume (GMV) and cortical thickness compared to nulliparous controls[1]. The left amygdala plays a crucial role in differentiating maternal and non-maternal brains[2]. These morphometric changes occur most dynamically within the first 6 weeks postpartum[2], likely mediated by sex steroid hormones and corticosteroids[3–6]. However, neocortical brain-structural alterations may not normalize to pre-pregnancy levels even by 12 weeks postpartum[2,7,8]. These changes suggest regionally specific short-term and long-term effects of pregnancy, childbirth, and motherhood on the brain. Although their biological role is not fully understood, they may be relevant for maternal attachment toward the offspring[2,7,9].

Given these morphological changes, aside with (i) the massive hormonal adaptations in the perinatal period[3,10], (ii) the reported hormonal regulation of brain connectivity[5,11,12], and (iii) the interactions between sex hormones and GABAergic as well as oxytonergic neurotransmission[13,14], it is to assume that brain function undergoes similar reorganization. Resting-state functional magnetic resonance imaging (rsfMRI) provides an effective, scalable approach to explore these changes, independent of participant compliance- or performance[15]. A prior rsfMRI study[16] reported alterations of default mode network (DMN) functional connectivity (FC) in postpartum mothers (one session between 1 and 4 months postpartum) compared to pre-conception. However, high-resolution follow-up data is needed to provide a clearer picture of the brain's functional reorganization during the early postpartum period, differentiating short-term biological impacts of pregnancy and early postpartum from those of motherhood[2]. For identifying biological mechanisms behind postpartum rsfMRI adaptations, voxel- or cluster-level MRI inferences are limited. Spatial colocalization analyses, which quantify alignment between (i) observed MRI maps and (ii) maps of a biological process or entity of interest[17–19] offer more detailed insights. This approach has been successfully used to study individual-level structural brain development[18] as well as rsfMRI alterations in Parkinson's and Huntington's disease[19,20].

We assessed healthy maternal brain function in a large baseline sample (n = 75), measured in their first postpartum week, and in a subgroup (n = 19) followed longitudinally at 3, 6, 9, 12, and finally 24 weeks (6 months) postpartum. Alongside MRI, we measured serum estradiol and progesterone levels and behavioral data at each session. We expected that, compared to a healthy nulliparous control group (NP, n = 23), postpartum women (PP) would show strong alterations of

rsfMRI metrics mapping intra- and interregional brain activity and FC. Our study design allowed for first insights into transitory and persistent natures of postpartum rsfMRI changes and to test for potential interactions with hormonal adaptations. For that, we (i) tested if whole-brain distributions of rsfMRI activity and connectivity changes colocalized spatially with hormone receptors and functionally related neurotransmitter receptors, and (ii) assessed if rsfMRI changes covaried with serum hormone levels over time. Additionally, we explored if enduring changes in brain function relate to psychological or behavioral shifts[2,7,9], particularly regarding mother-infant attachment and maternal depression.

2. Results

2.1. Demographic, hormonal, and psychological assessments

The baseline assessment was conducted on average 3.43 days postpartum (T0, SD = 2.03 days). The longitudinal subgroup was measured again at postpartum day 22.42 (T1, SD = 2.52), 43.57 (T2, SD = 3.06), 64.61 (T3, SD = 2.8), 84.91 (T4, SD = 3.71), and 173.32 (T5, SD = 10.15). Detailed sample characteristics are presented in Extended Data Tables 1–3. Postpartum and nulliparous groups differed in age at baseline (mean age = 30.52 vs. 28.04, SD = 3.54 vs. 4.91; Mann-Whitney-U-Test: $U = 1075.5$, $p < .001$; Extended Data Table 3).

We tested for longitudinal effects of hormone levels, psychological variables, and fMRI-derived measures using linear mixed models (LMM). We assessed the fixed effect of continuous postpartum week on each tested response variable, including random intercepts for each subject. For each response variable, two mixed linear models were calculated: (i) including only the linear postpartum week as fixed effect and (ii) including linear and quadratic effects. We found a quadratic effect of time on log-transformed progesterone levels, but not on estradiol or the estradiol/progesterone ratio. Maternal attachment (Maternal Postnatal Attachment Scale, MPAS)[21] and subclinical postpartum depression scores (Edinburgh Postnatal Depression Scale, EPDS)[22] showed linear and quadratic effects of time (nominal $p < .05$; Extended Data Table 3).

2.2. Strong regional alterations of resting-state activity and connectivity in the first postpartum week

To identify brain areas showing robust adaptation effects of pregnancy and childbirth, we followed a comprehensive rsfMRI analysis approach[23], simultaneously assessing postpartum

changes in voxel-level *intra*-regional/local rsfMRI activity (fractional amplitude of low frequency fluctuations, fALFF)[24], *intra*-regional/local FC (Local Correlation, LCOR), as well as *inter*-regional/global FC (Global Correlation, GCOR)[25]. To determine rsfMRI alterations occurring in the first postpartum week, we compared baseline postpartum and nulliparous groups in general linear models (GLM) controlling for age (non-parametric cluster-level inference[26]: voxel-level threshold $p < .01$, cluster-level threshold $p < .05$). We found two clusters with increased local activity (fALFF) in postpartum relative to nulliparous groups in right precentral and left medial temporal areas, and one cluster with decreased local activity in the right superior frontal gyrus. For LCOR, postpartum women showed decreased local connectivity in bilateral insulae compared to controls. In contrast, GCOR was decreased in the postpartum group relative to controls in bilateral putamen and pallidum (Table 1, Figure 1). In sensitivity analyses, results were robust against additional control for in-scanner motion, GMV, and education (Table S1).

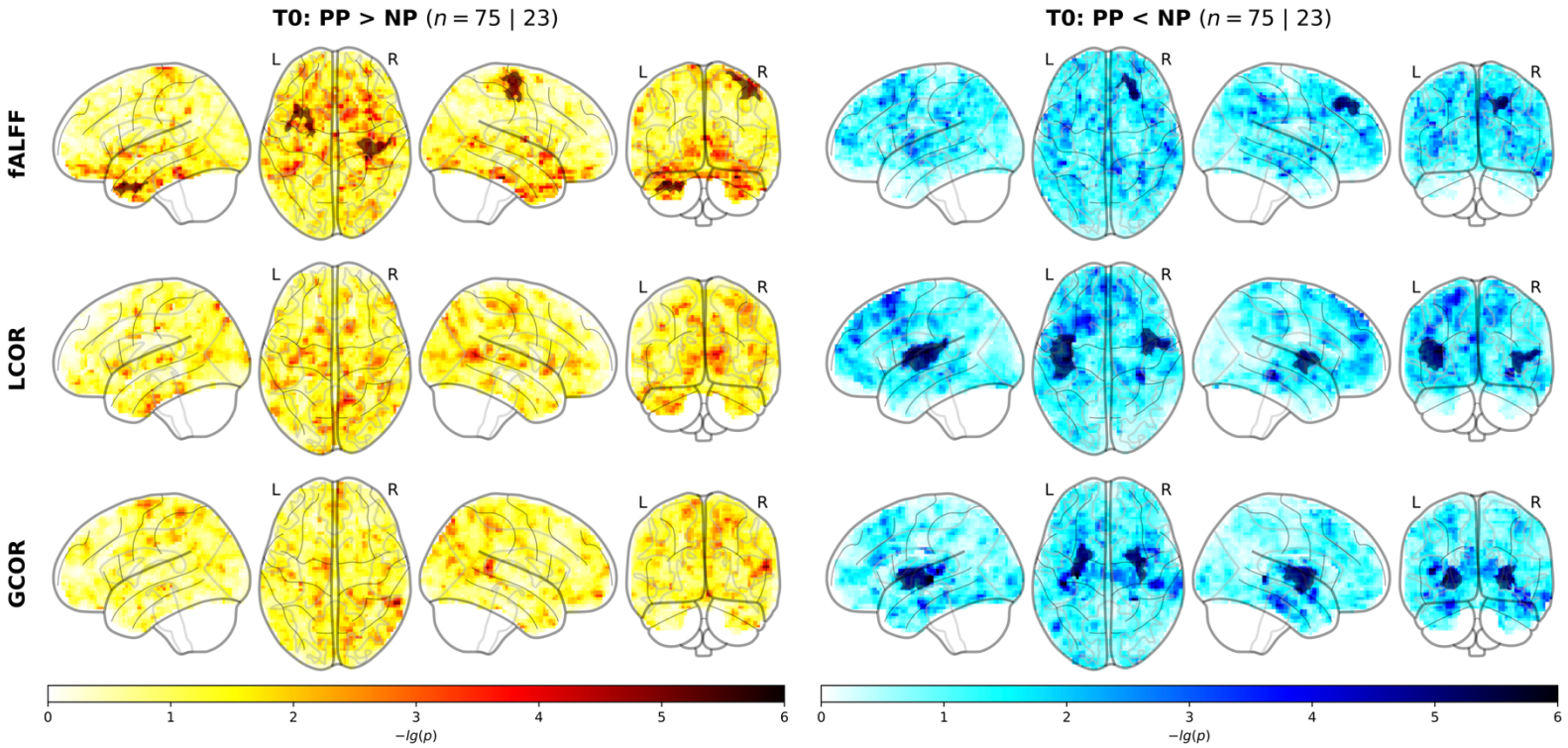

Figure 1. Clusters of differing local activity (fALFF), local connectivity (LCOR), and global connectivity (GCOR) in the nulliparous (NP) and postpartum (PP) groups at baseline.

Cluster-level and whole-brain results from baseline (T0) rsfMRI analyses. Brain maps for each rsfMRI metric (rows) and each contrast (columns) show voxel-level negative log10-transformed p values overlaid by cluster-level results in darker shades (non-parametric cluster mass permutation). Abbreviations: PP = postpartum, NP = nulliparous, fALFF = fractional amplitude of low frequency fluctuations, LCOR = local correlation, GCOR = global correlation.

Measure	Contrast	Cluster name	X	Y	Z	-lg(p)	Cluster size [mm^3]	AAL region coverage
fALFF	PP > NP	rightPrecentral	40	-20	60	1.43	3672	72.06% Precentral_R; 22.79% Postcentral_R
		leftMedTemp	-29	10	-36	1.37	3321	47.97% Temporal_Pole_Mid_L; 19.51% ParaHippocampal_L; 16.26% Temporal_Inf_L; 8.13% Temporal_Pole_Sup_L
	PP < NP	rightPFC	22	37	45	1.31	2835	80.95% Frontal_Sup_2_R; 14.29% Frontal_Mid_2_R
LCOR		leftIns	-41	-17	9	2.23	11124	36.89% Insula_L; 32.52% Rolandic_Oper_L; 9.95% Heschl_L; 7.77% Temporal_Sup_L
		rightIns	43	-2	6	1.44	5481	57.64% Insula_R; 25.62% Rolandic_Oper_R; 9.85% no_label
GCOR		leftPut	-26	-2	3	1.78	5724	71.23% Putamen_L; 20.28% Pallidum_L; 8.02% no_label
		rightPut	28	-5	3	1.6	5373	63.32% Putamen_R; 16.08% Pallidum_R; 13.57% no_label; 7.04% Insula_R

Table 1: Statistical and anatomical characteristics of baseline rsfMRI clusters.

Clusters were named after their main location. X, Y, and Z show coordinates in MNI-152 space. The non-parametric p value associated with each cluster based on its cluster mass is displayed negative log10 transformed. Clusters were characterized anatomically based on the AAL atlas in terms of the percentage to which each AAL region was contained in each cluster. Abbreviations: AAL = Automated Anatomic Labeling atlas, fALFF = fractional amplitude of low frequency fluctuations, LCOR = local correlation, GCOR = global correlation, PP = postpartum, NP = nulliparous, MED = medial, PFC = prefrontal cortex, Ins = insula, Put = putamen.

2.3. Temporal dissociation of intra- and interregional rsfMRI metrics in the postpartum period

To examine the longitudinal development of observed early postpartum rsfMRI changes, we extracted average rsfMRI signals from each significant baseline clusters. Independent t-tests at each time point were used to determine "normalization" of rsfMRI metrics relative to the control group and temporal trajectories were tested in LMMs with post-hoc paired t-tests. We found a general dissociation between local measures (fALFF and LCOR) and the global connectivity measure (GCOR) (Figure 2, Tables S2–4). *Intra*-regional neocortical alterations of activity and connectivity persisted across the 6 observed postpartum months. In contrast, reduced *inter*-regional whole-brain FC of subcortical areas showed normalization patterns, with no significant or visible group differences between postpartum and nulliparous groups at about 6-9 weeks postpartum (FDR-corrected). In line with that, only the GCOR clusters showed significant linear and quadratic longitudinal development (FDR-corrected). Controlling all analyses for underlying GMV reduced effect sizes while group differences and longitudinal trends remained stable (Tables S5–7). Specifically controlling only the significant longitudinal GCOR trajectories for influences of in-scanner motion, day of gestation, birth mode, baby weight or sex, breastfeeding, or total number of children did not affect the results (Table S8).

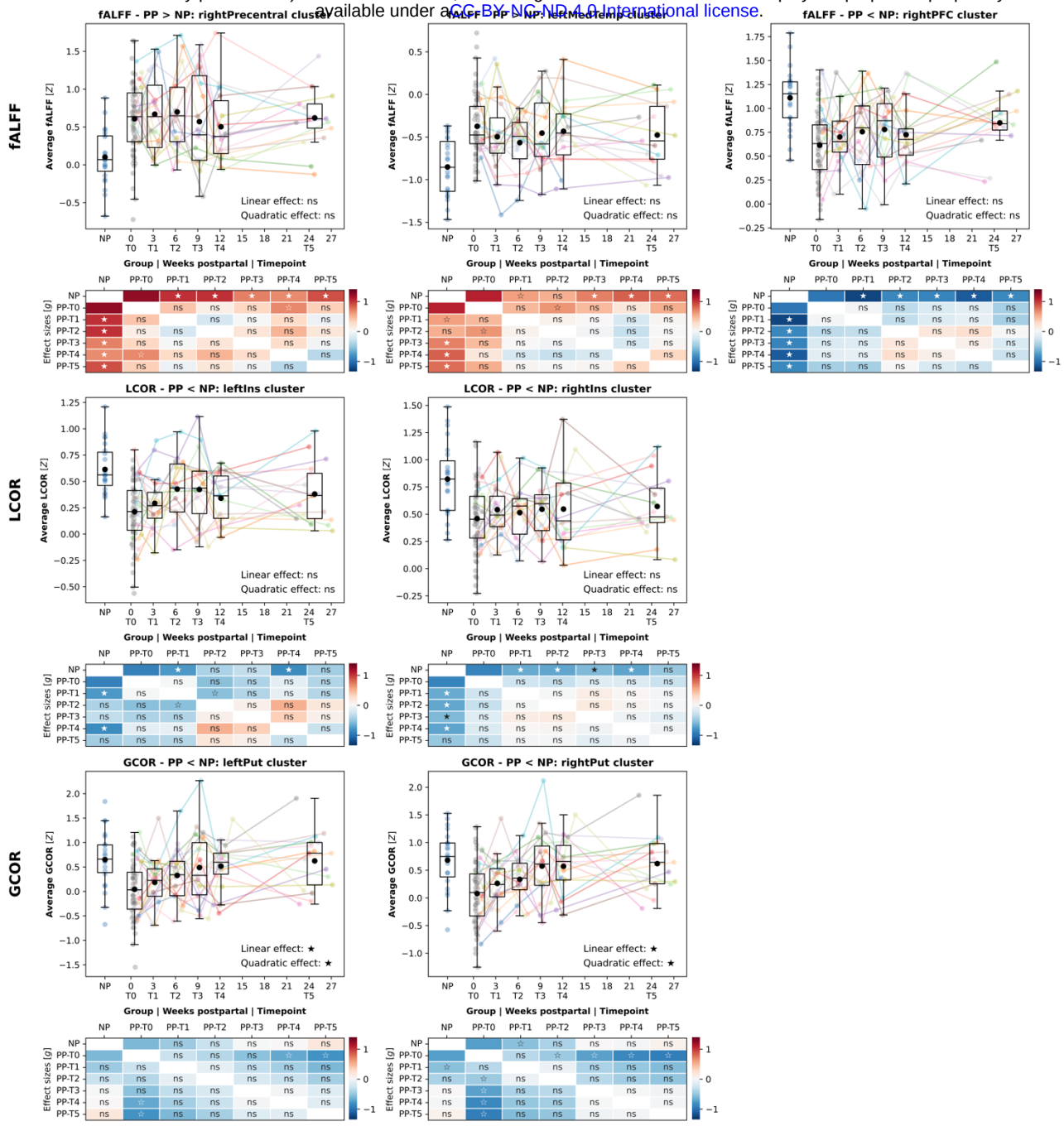

Figure 2: Longitudinal development of rsfMRI clusters.

Development of baseline cluster-wise averaged local and global connectivity and activity metrics across 6 postpartum months. Boxplots: x-axes show time in weeks postpartum (dimensional scale), y-axes show the Z-standardized rsfMRI metric. Each dot represents one subject at one individual time point, lines connect longitudinal scans. Boxplots show the distribution across subjects at each time point (black dot = mean, middle line = median, boxes = quartile 1 and 3, whiskers = range if below 1.5 * interquartile range from quartile 1 or 3). Heatmaps show effect sizes (Hedge's g) of within- and between-group comparisons, overlaid labels mark significances (filled star = false discovery-corrected, empty star = nominal $p < .05$, ns = $p > .05$. Significance of linear mixed models is printed in the lower left corner. Abbreviations: fALFF = fractional amplitude of low frequency fluctuations, LCOR = local correlation, GCOR = global correlation, PP = postpartum, NP = nulliparous, ns = not significant.

2.4. Whole-brain rsfMRI changes colocalize with potentially mediating biological systems

Assuming the change of a brain-functional metric is influenced by a brain system on another neurobiological level, the spatial distribution of this metric across the brain may colocalize with the biological system in question[18,20,27]. We therefore examined if postpartum rsfMRI changes and their normalization patterns after birth were distributed across the brain following spatial distributions of pregnancy-related hormonal receptors (progesterone: PGR, estrogen: ESR1/ESR2, cortisol: NR3C1/NR3C2) and functionally close neurotransmitter receptors (oxytocin: OXTR, GABA: $GABA_A$, glutamate: mGluR5). In-vivo maps of $GABA_A$ and mGluR5 distributions were obtained with positron emission tomography imaging in independent healthy adult subjects[28,29], all other maps were derived from postmortem Allen Brain Atlas data[30] (Figure 3, left). We tested for colocalization between (i) parcellated rsfMRI maps of each postpartum mother relative to the control group as a reference and (ii) independent receptor maps using Spearman correlations[31]. In case of a significant group-average colocalization at baseline (FDR-corrected), we evaluated the temporal development at each subsequent time point. Baseline postpartum changes of fALFF were positively colocalized with progesterone (FDR-corrected) and estrogen receptor distributions (nominal $p < .05$), but negatively colocalized with the metabotropic glutamate receptor distribution (FDR-corrected; Figure 3, upper right; Table S9). In line with cluster-level results reported above, both the fALFF-PGR and fALFF-mGluR5 colocalization persisted across the first 6 postpartum months (Figure 3, lower right; Table S9 and S10). LCOR changes showed spatial colocalization with estrogen, cortisol, and glutamate receptors (nominal $p < .05$). While GCOR changes colocalized positively with cortisol receptors (NR3C1: nominal, NR3C2: FDR) and $GABA_A$ (nominal), they colocalized negatively with progesterone and oxytocin receptors (FDR). Again, in line with the cluster-level results, these colocalization patterns normalized within the first 2 postpartum months.

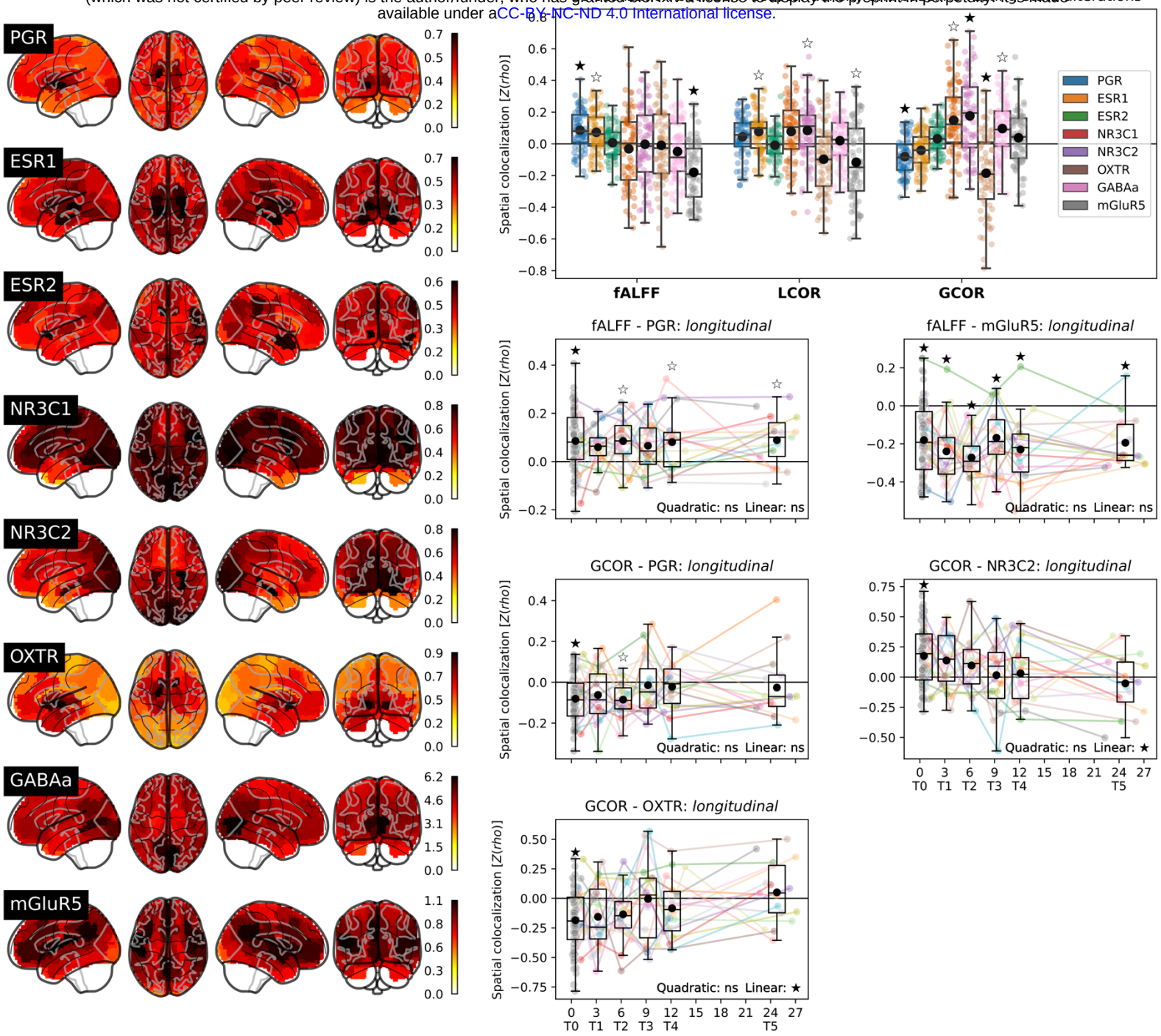

Figure 3: Subject-level spatial colocalization between postpartum rsfMRI alterations and hormonal/neurotransmitter receptor densities.

Left side: Parcellated and Z-standardized whole-brain hormone and neurotransmitter receptor distributions. Right side: Spatial colocalization analyses. Upper panel: Baseline analyses testing for colocalization between receptor distributions and rsfMRI data of each postpartum subject at baseline relative to the control group. X-axis: Z-transformed Spearman correlation coefficients, y-axis: rsfMRI metrics, colors: receptor maps. Lower panels: Longitudinal analyses following up on each baseline results if associated group permutation p values survived false discovery rate-correction (filled stars). The plot design equals Figure 2 with the y axis showing Z-transformed Spearman correlation coefficients. Abbreviations: fALFF = fractional amplitude of low frequency fluctuations, LCOR = local correlation, GCOR = global correlation, ns = not significant.

2.5. Receptor distributions provide a multivariate explanation of postpartum rsfMRI changes

To provide an easy-to-interpret quantification of the extent to which postpartum rsfMRI changes could be explained by hormone and neurotransmitter receptor distributions, we assessed the variance explained in multivariate linear regression analyses "predicting" baseline rsfMRI change patterns in individual postpartum mothers from receptor maps[17,18]. On average, baseline rsfMRI change patterns in PP were explained to 17.1% for fALFF (range 0–43.8%), 13.0% for LCOR (range 0–38.1%), and 18.3% for GCOR (0–44.0%).

2.6. Early postpartum normalization of global connectivity is not due to regression-to-the-mean effects

We further tested if normalization effects observed in GCOR-related variables were due to regression-toward-the-mean effects. For this, we (i) replicated baseline voxel-level GLM and spatial colocalization analyses while *excluding* the subjects with longitudinal data, (ii) extracted cluster-average data from subjects *with* longitudinal data using the clusters estimated on the independent cross-sectional sample, and (iii) tested for longitudinal linear and quadratic effects in the cluster-average data. The reduced postpartum sample (n = 56) showed the same bilateral putamen-related clusters of reduced global connectivity at baseline. Temporal development of the cluster-average data in independent longitudinal subjects followed similar trajectories as reported above. Baseline spatial colocalization patterns in the reduced sample were similar to those in the full sample (Extended Data Figure 1, Table S11).

2.7. Temporally dissociated intra- and interregional rsfMRI metric changes show diverging behavioral and hormonal association patterns

The temporal and spatial dissociation between postpartum alterations of local and global rsfMRI metrics indicates diverging underlying mechanisms. Given the strong hormonal fluctuations of the first postpartum weeks, it would be plausible if the observed transitory rsfMRI changes were hormone-related, while the long-lasting changes may be linked to more permanent behavioral or psychological adaptations following pregnancy and childbirth. Due to our rather small sample size, we conducted hormonal and behavioral association analyses on an exploratory level, evaluating general patterns rather than specific associations. To fully exploit our dense longitudinal data, we fitted LMMs testing for the interaction effect of postpartum weeks and MRI variables (cluster-level and spatial colocalization metrics) on both the behavioral and hormonal variables (hormone levels,

EPDS, and MPAS). We found two general patterns (Figure 4). First, GCOR-derived metrics seemed generally associated with hormone levels (Table S12), in line with the temporal development observed in GCOR-related variables and indicating that postpartum adaptations of long-range connectivity could be driven by changes in corticosteroid hormones. In contrast, postpartum depression symptoms (EPDS) and mother-child attachment (MPAS) seemed more associated with local resting-state metrics, suggesting a potential behavioral correlate for persistent changes in postpartum brain function (Table S13). We maintain, however, that these findings are of a preliminary nature and would require targeted evaluation in an independent sample.

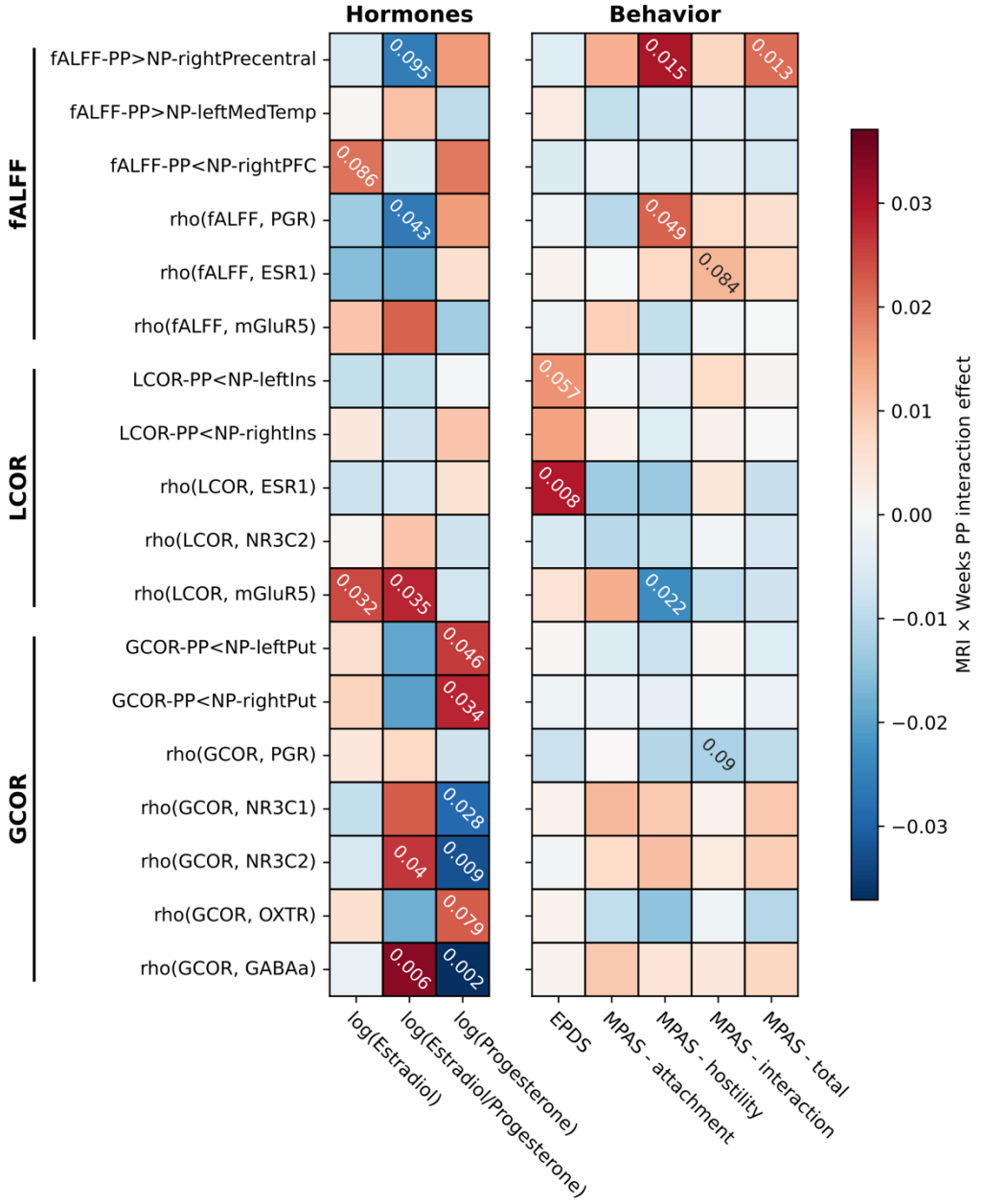

Figure 4: Patterns of association over time between rsfMRI results and hormone levels as well as behavior.

Results of linear mixed models to determine time-dependent covariation between rsfMRI metrics (cluster-level and spatial colocalization estimates) and hormone levels (left) as well as mother-child attachment and postpartum depression symptoms (right). Heatmap colors represent standardized effect sizes of the MRI x postpartum week interaction effect. Overlaid labels show nominal p values ($p < 0.1$). The shown analyses are intended to identify general patterns of associations, rather than interpreting specific tests. Abbreviations: fALFF = fractional amplitude of low frequency fluctuations, LCOR = local correlation, GCOR = global correlation, PP = postpartum, NP = nulliparous, MPAS = Maternal Postnatal Attachment Scale, EPDS = Edinburgh Postnatal Depression Scale.

3. Discussion

In this study, we tracked postpartum reorganization of brain function in a group of healthy mothers followed from shortly after birth until 6 months postpartum. While neocortical intraregional resting-state activity and connectivity alterations persisted throughout the study time period, interregional connectivity of subcortical areas normalized to control levels within the first 2 postpartum months. Preliminary evidence suggested that this normalization was related to adaptations of the steroid hormone system, while persistent resting-state changes might show associations to maternal behavior. Whole-brain rsfMRI change patterns were partly explained by distributions of corticosteroid and related neurotransmitter systems across brain regions, suggesting biological targets for future research.

The *(sub-)acute postpartum period*, defined a first 6 postpartum weeks, is marked by extensive physiological and hormonal adaptations[32]. Strongly decreased bilateral putamen FC in postpartum women and its normalization during the subacute postpartum period in interaction with progesterone blood levels suggest effects of progesterone on neural function, in line with progesterone-specific and general corticosteroid effects on basal ganglia morphology and function[33,34]. Supporting this relationship beyond the brain-regional level, postpartum inter-regional connectivity changes colocalized negatively with the progesterone receptor across brain regions (*less* FC in areas with *higher* progesterone receptor gene expression), as well normalizing within weeks. Previous research suggested that the post-childbirth drop in progesterone and its metabolites might be involved in the development of baby blues and postpartum depression trough dysregulated GABAergic neurotransmission[35]. The specific effect on a rsfMRI metric indicates a worthwhile target for future research on postpartum depression. However, it is important to note that despite postpartum physiological adaptations are significant, it is unclear if and to which extent these affect the mental health of most postpartum mothers. Genetic predisposition and life experiences likely contribute to the individual risk of developing mood disorders in the face of strong hormonal fluctuations[36]. Future studies in populations at risk for postpartum depression can build on our findings to identify clinically valuable biomarkers.

It remains unclear when the post-pregnancy recovery of the maternal brain is completed and if pregnancy has long-lasting neural effects. Structural changes begin early in the postpartum phase[37,38], lasting up to 6 months[37] or even longer[7,39]. We found persistent changes in local activity of motor, medial temporal, and prefrontal cortices, as well as of local FC in the bilateral insulae. Across brain regions, these changes were strongest in areas with higher progesterone and estrogen

receptor gene expression and lowest in areas with higher glutamate receptor density, possibly indicating underlying biological mechanisms requiring further evaluation. Notably, we found no normalization patterns in local activity metrics but early evidence of associations with postnatal physiological and behavioral changes. Especially the potential association between insular connectivity and mother-child attachment requires further investigation[40,41]. Hoekzema et al.[16] reported long-term effects of pregnancy or motherhood on resting-state connectivity within the DMN, a direct comparison to our findings is limited due to major difference in the covered peripartum time period and analysis methodology. Our rsfMRI data, however, aligns with those of Hoekzema et al. in the aspect that both datasets indicated associations of resting-state changes months after birth to mother-child bonding. Here, one could assume that the experience of motherhood influences the maternal brain, as for example observed for time-sensitive relationships between postpartum amygdala volume and hostile behavior toward the child[2] as well as for protective neural effects of parenting[8].

Several limitations of this study should be pointed out, most importantly the small size of the longitudinal subsample and the lack of a longitudinal follow-up in the control group, posing the risk of especially complex statistical models being underpowered. However, we consider the comparisons with the nulliparous group to be robust, as relevant changes in controls are unlikely given the relatively short follow-up duration. Due to the lack of pre-pregnancy and during-pregnancy rsfMRI, we cannot disentangle the effects of pregnancy from those of postpartum adaptation or preexisting factors. Especially behavioral and hormonal association patterns found in this study require replicated in larger groups and should be assessed in postpartum and control participants alike. Finally, the inferences from spatial colocalization analyses are limited by their reliance on heterogeneous external datasets, which was acquired partly from mostly male postmortem samples. Care is needed when interpreting colocalization analyses with bulk-sequencing post-mortem gene expression atlases as it is unclear to which extent these data correspond to actual protein activity[42].

3.1. Conclusion and future outlook

We provide evidence of dynamic functional adaptation processes in the early postpartum brain. While the subcortex-centered global connectivity changes may be of transient nature and are related to hormonal adaptations, neocortical brain activity and connectivity show persistent alterations, possibly associated with behavioral and psychological processes. Building on our data, fur-

ther longitudinal studies involving larger cohorts and pre-pregnancy assessments will bring valuable insights into the post-childbirth recovery of pregnancy-affected brain morphology and function. Along with longitudinal multimodal neuroimaging, cognitive and lifestyle assessments, the tracking of ovarian hormones from before pregnancy through the postpartum phase will help identify factors contributing to the phenomena observed in this study. It is imperative to understand the long-term effects of pregnancy-related adaptations, which, in addition to playing a protective role, may also render women more vulnerable to certain risks. It needs to be ascertained if these changes contribute to the development of psychiatric conditions, especially in women at higher risks for postpartum psychiatric disorders.

4. Methods

4.1. Study samples

Postpartum women were recruited in the Department of Gynecology and Obstetrics, University Hospital Aachen, Germany, within two studies run in parallel by the Department for Psychiatry, Psychotherapy, and Psychosomatics at the same hospital. Both studies were led by the same investigators and applied the same testing protocols for MRI, hormonal, and behavioral measurements. Study 1 targeted early postpartum brain changes with a focus on early prediction of postpartum depression[43]. Cross-sectional morphological data was published in Chechko et al. (2022)[1]. In Study 2, a healthy subgroup of women recruited for Study 1 (no psychiatric diagnosis, no risk factors, narrow age span) was followed up for a longitudinal exploration of specific aspects of the postpartum period. Longitudinal morphological changes and their behavioral associations up to postpartum week 12 were assessed in Nehls et al. (2023)[2]. Additionally, a nulliparous control sample was recruited for baseline comparison, scanned once at the same scanner. While our prior studies took a psychological viewpoint, focusing on psychopathological and behavioral correlates of postpartum brain changes, here we approached the topic from a physiological perspective, using the dense 6-months longitudinal data to gain insights into biological mechanisms underlying these neural adaptations.

The current baseline sample (T0) consisted of 75 non-depressed postpartum women from Study 1, recruited within 1 to 7 days of delivery. From this sample, recruited for Study 2, 19 PP women took part in longitudinal MRI assessments, with measurements at 3 weeks (T1, n = 19), 6 weeks (T2, n = 18), 9 weeks (T3, n = 19), 12 weeks (T4, n = 19) and 24 weeks (T5, n = 17) postpartum.

At each time point, blood samples were drawn to determine blood plasma levels of estradiol and progesterone. PP participants were assessed for symptoms of postpartum depression by means of the Edinburgh Postnatal Depression Scale (EPDS; T0–T5; total score)[22] and for mother-child attachment through the Maternal Postnatal Attachment Scale (MPAS; T1–T5; total score and subscores for quality of attachment, absence of hostility, and pleasure in interaction). The control group consisted of 23 healthy nulliparous women with no history of psychiatric disorders. Prior to enrolment in both studies, written informed consent was obtained from each participant. After excluded sessions that exceeded motion cut-offs and did not pass visual quality control (n = 1 with MRI data reconstruction failure), the final dataset consisted of data from 98 subjects (PP = 75, NP = 23) with overall 189 sessions (longitudinal: T0: 19, T1: 19, T2: 18, T3: 19, T4: 18, T5: 17).

4.2. Hormonal assays

Progesterone and estradiol serum concentrations were measured before each scanning session and analyzed by competitive immunometry electrochemistry luminescence detection at the Laboratory Diagnostic Center, University Hospital RWTH Aachen, Germany. The samples were run on a Roche Cobas e601 and on a Roche Cobas e801 with Cobas Elecsys estradiol and progesterone reagent kits, respectively (Roche Diagnostics, Bromma, Sweden). For progesterone, the measurement interval was .05–60 ng/ml with an intra-assay coefficient of variation of 2.33–2.49%. For estradiol, the measurement interval was 5–3000 pg/ml with a coefficient of variation of 1.77–2.91%.

4.3. Software, external data sources, and code availability

Processing of functional and structural images was conducted in a MATLAB (R2022a) environment using CONN (21a)[44], building on SPM12 routines. Statistical analyses were calculated in a Python (3.9.12) environment using Nilearn (0.10.0)[45] for voxel-wise rsfMRI group comparisons. Resulting spatial clusters were characterized using atlasreader (0.1.2)[46]. Spatial colocalization estimates were calculated in JuSpyce (0.0.3)[31]. All post-hoc statistical analyses were conducted with statsmodels (0.13.5) and pingouin (0.5.3)[47,48]. Brain gene expression and nuclear imaging data were obtained with abagen (0.1.3)[49], neuromaps (0.0.3)[50], and from author sources[28,29]. Visualizations were created with matplotlib (3.5.2)[51], seaborn (0.12.1)[52], and Nilearn.

The analysis code, organized in a Jupyter notebook, is available as a supplement. Due to privacy protection, we cannot provide subject data openly. All group-level results are provided in

supplementary tables. Group-level MRI volumes will be uploaded to Neurovault following publication.

4.4. MRI acquisition and processing

All participants were scanned at the same Siemens Magnetom Prisma 3T MRI scanner. MRI Structural T1-weighted images were acquired using a Rapid Acquisition Gradient Echo sequence with following parameters: TR = 2300 ms, TE = 1.99 ms, FoV = 256 x 256 mm, number of slices = 176, voxel size = 1 x 1 x 1 mm^3. For rsfMRI, all probands underwent a 6.6 minutes gradient-echo Echo Planar Imaging protocol with TR = 2200 ms, TE = 30 ms, flip-angle = 90 °, FoV = 200 x 200 mm, number of slices = 36, number of volumes = 300, voxel-size = 3.1 x 3.1 x 3.1 mm^3.

Preprocessing of functional images consisted of removal of the first four frames, realignment for motion correction, and co-registration to structural images with subsequent spatial normalization into Montreal Neurological Institute space using parameters derived from structural data. The normalization parameters were applied with modulation to segmented gray matter probability maps to obtain corresponding voxel-wise GMV. Functional and structural images were interpolated to 3-mm and 1-mm isotopic resolution, respectively. A Gaussian smoothing kernel of 6-mm full width at half maximum was applied to rsfMRI data. Twenty-four motion parameters along with mean white matter and cerebrospinal fluid signals were regressed out of the functional data[53]. The resulting images were linearly detrended and temporally bandpass filtered (.01–.08 Hz). A gray matter mask (probability > .2) was applied to all images to restrict analyses to gray matter tissue. For spatial colocalization analyses, data were parcellated into 100 cortical and 16 subcortical parcels[54,55]. All structural and functional MRI volumes before and after preprocessing were visually quality-controlled and subject exceeding motion cut-offs of a mean and maximum framewise displacement of 0.5 and 3 mm were excluded.

4.5. RsfMRI analyses at baseline

We assessed postpartum changes of voxel-level intraregional/local rsfMRI activity (fALFF) and connectivity (LCOR) as well as interregional/global connectivity (GCOR). For descriptions of these metrics, please refer to Lotter et al.[23]. To identify spatial clusters of altered regional functional connectivity and activity in mothers after childbirth, we compared voxel-wise metrics between the baseline PP and NP groups. We fitted GLMs including age as a covariate.

Cluster-level significance was determined in separate positive (PP > NP) and negative contrasts (PP < NP) based on permutation of cluster masses (10,000 iterations) using a voxel-level threshold of $p < .01$ and a cluster-level threshold of $p < .05$[26].

4.6. Longitudinal rsfMRI analyses

To assess how rsfMRI changes at baseline developed during the first 6 postpartum months**,** we extracted average rsfMRI data for each cluster and assessed (i) differences between PP and NP at each time point using ANCOVAs controlled for age, (ii) longitudinal development in PP using LMMs, and (iii) within-subject differences between time points in multiple paired t-tests. FDR-correction was applied to all p values resulting from each analysis (separately for step i, ii, and iii). LMMs were designed to assess the fixed effect of postpartum week on each MRI metric, while accounting for within-subject variance. In sensitivity analyses, we included average gray matter signals within the same clusters, as extracted from modulated gray matter maps as covariates[23].

4.7. Spatial colocalization between voxel-wise rsfMRI changes and receptor distributions

We examined whether changes of rsfMRI metrics in PP relative to NP appeared in patterns across the brain resembling functionally related receptor distributions[27], indicating potential mechanistic relationships[20,27]. We first assessed if the mean spatial colocalization of rsfMRI changes in PP at baseline exceeded those of permutated data. RsfMRI-receptor combinations that showed significant colocalization at baseline were followed up in the longitudinal data.

Corticosteroid hormone and oxytocin receptor maps (PGR, ESR1/ESR2, NR3C1/NR3C2, OXTR) were constructed from postmortem Allen Brain Atlas gene expression data (1 female, ages 24.0–57.0 years, mean = 42.50, SD = 13.38) [30] in 116-region volumetric atlas space. The abagen toolbox was used for map construction, while applying bilateral mirroring across hemispheres. GABAergic ($GABA_A$) and glutamatergic (mGluR5) receptor maps were obtained with positron emission tomography from independent groups of healthy adult subjects ($GABA_A$: [11C]flumazenil, n = 10, mean = 26.60, SD = 7.00 years; mGluR5: [11C]ABP688, n = 73, mean = 19.90, SD = 3.04 years).

Spatial relationships were tested for by (i) parcellating all rsfMRI and receptor data in 116 cortical and subcortical parcels, (ii) calculating parcel-wise rsfMRI Z scores for each PP subject at a given time point by subtraction of the mean rsfMRI metric in NP subjects and division by the NP standard deviation, (iii) correlating these subject-level 116-parcel Z score maps with each receptor

map using Spearman correlations, (iv) generating a null distribution of Spearman correlation coefficients by repeating this process after permuting the PP-NP labels, and (v) fitting a Gaussian curve to these null distributions to estimate the p value of each observed Spearman correlation ("colocalization") coefficient. The concept was described in detail in Dukart et al.[27] and implemented via JuSpyce[31]. The Gaussian curve was fitted to generate p values with enough decimal places to accurately apply FDR correction. If significant colocalization was observed on the group level at baseline, the longitudinal development of these colocalization metrics was tested for using LMMs as described above. In spatial colocalization analyses, it is important to control for spatial autocorrelation patterns present in most brain maps. We assume that the group permutation approach is robust against these confounds, as the receptor map spatial autocorrelation likely influenced both the observed and the null colocalization estimates to similar degrees.

Additionally, to quantify the extent to which whole-brain rsfMRI changes in PP at baseline were explained by the receptor maps in an easily interpretable way, we fitted multivariate linear models "predicting" subject-wise rsfMRI changes in PP from all receptor maps as independent variables[18,56]. We quantified the outcome as the average adjusted R^2 across the PP sample.

4.8. Analyses of MRI, hormone, and behavior associations

To evaluate potential physiological and behavioral correlates of temporal trajectories observed in the rsfMRI data, we fitted LMMs evaluating the MRI metric vs. weeks postpartum interaction effect on hormonal and behavioral variables (log-transformed progesterone, estrogen, and progesterone/estrogen ratio, as well as MPAS and EPDS total scores and MPAS sub-scale scores). Given the small longitudinal sample size, these analyses were conducted on an exploratory level, evaluating patterns rather than specific associations. To allow for this, results where visualized as a heatmap focusing on effect sizes.

5. References

1. Chechko, N. *et al.* The expectant brain–pregnancy leads to changes in brain morphology in the early postpartum period. *Cerebral Cortex* **32**, 4025–4038 (2022).
2. Nehls, S., Losse, E., Enzensberger, C., Frodl, T. & Chechko, N. Time-sensitive changes in the maternal brain and their influence on mother-child attachment. *Translational Psychiatry* (2023).
3. Galea, L. A. M. & Frokjaer, V. G. Perinatal depression: embracing variability toward better treatment and outcomes. *Neuron* **102**, 13–16 (2019).
4. Sacher, J., Chechko, N., Dannlowski, U., Walter, M. & Derntl, B. The peripartum human brain: Current understanding and future perspectives. *Frontiers in Neuroendocrinology* **59**, 100859 (2020).

5. Pritschet, L. *et al.* Functional reorganization of brain networks across the human menstrual cycle. *NeuroImage* **220**, 117091 (2020).
6. Zsido, R. G. *et al.* Ultra-high-field 7T MRI reveals changes in human medial temporal lobe volume in female adults during menstrual cycle. *Nat. Mental Health* **1**, 761–771 (2023).
7. Hoekzema, E. *et al.* Pregnancy leads to long-lasting changes in human brain structure. *Nature Neuroscience* **20**, 287–296 (2017).
8. Orchard, E. R. *et al.* Neuroprotective effects of motherhood on brain function in late life: A resting-state fMRI study. *Cerebral Cortex* **31**, 1270–1283 (2021).
9. Kim, P. *et al.* The plasticity of human maternal brain: Longitudinal changes in brain anatomy during the early postpartum period. *Behavioral Neuroscience* **124**, 695–700 (2010).
10. Lindsay, J. R. & Nieman, L. K. The hypothalamic-pituitary-adrenal axis in pregnancy: Challenges in disease detection and treatment. *Endocrine Reviews* **26**, 775–799 (2005).
11. Peper, J. S., van den Heuvel, M. P., Mandl, R. C. W., Pol, H. E. H. & van Honk, J. Sex steroids and connectivity in the human brain: A review of neuroimaging studies. *Psychoneuroendocrinology* **36**, 1101–1113 (2011).
12. Andreano, J. M., Touroutoglou, A., Dickerson, B. & Barrett, L. F. Hormonal Cycles, Brain Network Connectivity, and Windows of Vulnerability to Affective Disorder. *Trends in Neurosciences* **41**, 660–676 (2018).
13. Barth, C., Villringer, A. & Sacher, J. Sex hormones affect neurotransmitters and shape the adult female brain during hormonal transition periods. *Frontiers in Neuroscience* **9**, 37 (2015).
14. Ivell, R. & Walther, N. The role of sex steroids in the oxytocin hormone system. *Molecular and cellular endocrinology* **151**, 95–101 (1999).
15. Damoiseaux, J. S. *et al.* Consistent resting-state networks across healthy subjects. *Proceedings of the National Academy of Sciences* **103**, 13848–13853 (2006).
16. Hoekzema, E. *et al.* Mapping the effects of pregnancy on resting state brain activity, white matter microstructure, neural metabolite concentrations and grey matter architecture. *Nature Communications* **13**, 6931 (2022).
17. Hansen, J. Y. *et al.* Mapping neurotransmitter systems to the structural and functional organization of the human neocortex. *Nature Neuroscience* **25**, 1569–1581 (2022).
18. Lotter, L. D. *et al.* Human cortex development is shaped by molecular and cellular brain systems. *bioRxiv : the preprint server for biology* (2023) doi:10.1101/2023.05.05.539537.
19. Dukart, J. *et al.* JuSpace : A tool for spatial correlation analyses of magnetic resonance imaging data with nuclear imaging derived neurotransmitter maps. *Human Brain Mapping* **42**, 555–566 (2021).
20. Kasper, J. *et al.* Local synchronicity in dopamine-rich caudate nucleus influences Huntington's disease motor phenotype. *Brain* (2023) doi:10.1093/brain/awad043.
21. Condon, J. T. & Corkindale, C. J. The assessment of parent-to-infant attachment: development of a self-report questionnaire instrument. *Journal of Reproductive and Infant Psychology* **16**, 57–76 (1998).
22. Cox, J. L., Holden, J. M. & Sagovsky, R. Detection of postnatal depression. Development of the 10-item Edinburgh Postnatal Depression Scale. *The British Journal of Psychiatry* **150**, 782–786 (1987).
23. Lotter, L. D. *et al.* Recovery-Associated Resting-State Activity and Connectivity Alterations in Anorexia Nervosa. *Biological Psychiatry: Cognitive Neuroscience and Neuroimaging* **6**, 1023–1033 (2021).
24. Zou, Q.-H. *et al.* An improved approach to detection of amplitude of low-frequency fluctuation (ALFF) for resting-state fMRI: fractional ALFF. *Journal of neuroscience methods* **172**, 137–141 (2008).

25. Whitfield-Gabrieli, S. & Nieto-Castanon, A. Conn : A Functional Connectivity Toolbox for Correlated and Anticorrelated Brain Networks. *Brain Connectivity* **2**, 125–141 (2012).
26. Eklund, A., Nichols, T. E. & Knutsson, H. Cluster failure: Why fMRI inferences for spatial extent have inflated false-positive rates. *Proceedings of the National Academy of Sciences* **113**, 7900–7905 (2016).
27. Dukart, J. *et al.* JuSpace : A tool for spatial correlation analyses of magnetic resonance imaging data with nuclear imaging derived neurotransmitter maps. *Human Brain Mapping* **42**, 555–566 (2021).
28. Kaulen, N. *et al.* mGluR5 and GABAA receptor-specific parametric PET atlas construction—PET/MR data processing pipeline, validation, and application. *Human Brain Mapping* **43**, 2148–2163 (2022).
29. Smart, K. *et al.* Sex differences in [11 C]ABP688 binding: a positron emission tomography study of mGlu5 receptors. *European Journal of Nuclear Medicine and Molecular Imaging* **46**, 1179–1183 (2019).
30. Hawrylycz, M. J. *et al.* An anatomically comprehensive atlas of the adult human brain transcriptome. *Nature* **489**, 391–399 (2012).
31. Lotter, L. D. & Dukart, J. JuSpyce - a toolbox for flexible assessment of spatial associations between brain maps. *2022* doi:10.5281/zenodo.6884932.
32. Romano, M., Cacciatore, A., Giordano, R. & La Rosa, B. Postpartum period: three distinct but continuous phases. *Journal of prenatal medicine* **4**, 22–5 (2010).
33. Pletzer, B., Harris, T.-A., Scheuringer, A. & Hidalgo-Lopez, E. The cycling brain: menstrual cycle related fluctuations in hippocampal and fronto-striatal activation and connectivity during cognitive tasks. *Neuropsychopharmacology* **44**, 1867–1875 (2019).
34. Macoveanu, J. *et al.* Sex-steroidhormone manipulation reduces brain response toreward. *Neuropsychopharmacology 2016 41:4* **41**, 1057–1065 (2015).
35. Cutler, A. J., Mattingly, G. W. & Maletic, V. Understanding the mechanism of action and clinical effects of neuroactive steroids and GABAergic compounds in major depressive disorder. *Translational Psychiatry* **13**, 228 (2023).
36. Steiner, M., Dunn, E. & Born, L. Hormones and mood: From menarche to menopause and beyond. *Journal of Affective Disorders* **74**, 67–83 (2003).
37. Oatridge, A. *et al.* Change in brain size during and after pregnancy: study in healthy women and women with preeclampsia. *American Journal of Neuroradiology* **23**, 19–26 (2002).
38. Luders, E. *et al.* From baby brain to mommy brain: Widespread gray matter gain after giving birth. *Cortex* **126**, 334–342 (2020).
39. Martínez-García, M. *et al.* Do Pregnancy-Induced Brain Changes Reverse? The Brain of a Mother Six Years after Parturition. *Brain Sciences* **11**, 1–14 (2021).
40. Rocchetti, M. *et al.* Neurofunctional maps of the 'maternal brain' and the effects of oxytocin: A multimodal voxel-based meta-analysis. *Psychiatry and Clinical Neurosciences* **68**, 733–751 (2014).
41. Morawetz, C., Bode, S., Derntl, B. & Heekeren, H. R. The effect of strategies, goals and stimulus material on the neural mechanisms of emotion regulation: A meta-analysis of fMRI studies. *Neuroscience & Biobehavioral Reviews* **72**, 111–128 (2017).
42. Liharska, L. E. *et al.* A study of gene expression in the living human brain. 2023.04.21.23288916 Preprint at https://doi.org/10.1101/2023.04.21.23288916 (2023).
43. Schnakenberg, P. *et al.* Examining early structural and functional brain alterations in postpartum depression through multimodal neuroimaging. *Sci Rep* **11**, 13551 (2021).
44. Whitfield-Gabrieli, S. & Nieto-Castanon, A. Conn: a functional connectivity toolbox for correlated and anticorrelated brain networks. *Brain connectivity* **2**, 125–141 (2012).

45. Abraham, A. *et al.* Machine learning for neuroimaging with scikit-learn. *Frontiers in Neuroinformatics* **8**, (2014).
46. Notter, M. *et al.* AtlasReader: A Python package to generate coordinate tables, region labels, and informative figures from statistical MRI images. *Journal of Open Source Software* **4**, 1257 (2019).
47. Seabold, S. & Perktold, J. Statsmodels: Econometric and Statistical Modeling with Python. in 92–96 (2010). doi:10.25080/Majora-92bf1922-011.
48. Vallat, R. Pingouin: statistics in Python. *Journal of Open Source Software* **3**, 1026 (2018).
49. Markello, R. D. *et al.* Standardizing workflows in imaging transcriptomics with the abagen toolbox. *eLife* **10**, (2021).
50. Markello, R. D. *et al.* Neuromaps: structural and functional interpretation of brain maps. *Nature Methods* **19**, 1472–1479 (2022).
51. Hunter, J. D. Matplotlib: A 2D Graphics Environment. *Computing in Science & Engineering* **9**, 90–95 (2007).
52. Waskom, M. seaborn: statistical data visualization. *Journal of Open Source Software* **6**, 3021 (2021).
53. Friston, K. J., Williams, S., Howard, R., Frackowiak, R. S. J. & Turner, R. Movement-Related effects in fMRI time-series. *Magnetic Resonance in Medicine* **35**, 346–355 (1996).
54. Schaefer, A. *et al.* Local-Global Parcellation of the Human Cerebral Cortex from Intrinsic Functional Connectivity MRI. *Cerebral Cortex* **28**, 3095–3114 (2018).
55. Tian, Y., Margulies, D. S., Breakspear, M. & Zalesky, A. Topographic organization of the human subcortex unveiled with functional connectivity gradients. *Nature Neuroscience* **23**, 1421–1432 (2020).
56. Hansen, J. Y. *et al.* Mapping neurotransmitter systems to the structural and functional organization of the human neocortex. *Nature Neuroscience* **25**, 1569–1581 (2022).

6. Data sharing

The data that support the findings of this study are available from the corresponding author, NC, upon reasonable request.

7. Acknowledgments and Funding

The study was funded by the Rotation Program (2015–2017) of the Medical Faculty, University Hospital RWTH Aachen, and the Deutsche Forschungsgemeinschaft (DFG; 410314797 and 512021469). Leon D. Lotter received financial support from the Max Planck Society (MPG) and the German Ministry of Education and Research (BMBF), Germany. This work was supported by the Brain Imaging Facility of the Interdisciplinary Center for Clinical Research (IZKF) Aachen within the Faculty of Medicine at RWTH Aachen University.

8. Competing interests

The authors declare no competing interests.

9. Author contribution

Conceptualization: NC, SN. Data Curation: NC, SN, EL. Formal Analyses: LL. Funding acquisition: NC. Investigation: NC, SN, EL. Methodology: JD, LL. Project administration: NC, SN. Supervision: NC, JD. Visualization: LL. Writing – original draft: NC, LL. Writing - review and editing: all authors. All authors confirm that they had full access to all data in the study and accept responsibility to submit for publication.

10. Extended Data

	Nulliparous (NP)						Postpartum (PP)						MWU-test	
	count	mean	std	min	50%	max	count	mean	std	min	50%	max	U	p
Age	23	28.04	4.91	20	28	36	75	30.52	3.54	21	31	39	1075.5	0.001
Education	19	3.53	0.51	3	4	4	73	3.38	0.92	0	4	5	1418.5	0.489
Mean FWD	23	0.16	0.04	0.09	0.17	0.25	75	0.18	0.08	0.05	0.16	0.4	1877	0.898
Max FWD	23	0.54	0.27	0.19	0.44	1.38	75	0.69	0.4	0.17	0.55	2.06	1519	0.113
Weeks postpartum							75	0.49	0.29	0.14	0.43	1.43		
Days of gestation							75	274.85	11.83	238	277	294		
Child's birth weight							75	3250.2	474.5	2050	3280	4290		

Extended Data Table 1: Baseline sample characteristics (dimensional).

Data was compared using Mann-Whitney-U-tests. Abbreviations: FWD = frame-wise displacement, std = standard deviation, MWU = Mann-Whitney-U-test.

Variable	Group	Category	Count
Country of origin	Nulliparous	Bulgaria	1
		China	1
		Germany	13
		France	1
		Iran	1
		Italy	1
		Switzerland	1
	Postpartum	Belgium	1
		Germany	45
		Liberia/Ghana	1
		Lithuania	1
		Netherlands	1
		Poland	2
		Russia	1
		Slovakia	1
		Spain	1
		Tajikistan	1
		Germany	1
Baby blues	Postpartum	no	37
		yes	38
Sex of baby		female	35
		male	40
Birth mode		emergency	6
		section	19
		spontaneous	47
		ventouse	3
Breastfeeding		no	9
		yes	66
Number of children		1	50
		2	23
		3	2
Hormonal contraception	Nulliparous	no	15
		yes	4
	Postpartum	no	0
		yes	0

Extended Data Table 2: Baseline sample characteristics (categorical).

Variable	Postpartum (PP): T0			Postpartum (PP): T1			Postpartum (PP): T2			Postpartum (PP): T3			Postpartum (PP): T4			Postpartum (PP): T5			LMM	Weeks PP			Weeks PP^2		
	count	mean	std	count	mean	std	count	mean	std	count	mean	std	count	mean	std	count	mean	std	df	converged	coef	p	converged	coef	p
Weeks postpartum	19	0.86	0.32	19	3.2	0.36	18	6.23	0.45	19	9.23	0.4	18	12.13	0.53	17	24.76	1.45								
EPDS	19	6.37	4	19	6.42	4.99	18	5.33	3.68	19	4.53	3.22	18	3.56	2.96	13	4	3.51	(3, 104)	TRUE	-0.116	0.001	TRUE	0.01	0.017
MPAS - total	0			19	81.32	10.25	18	83.61	8.29	19	83	8.83	18	82.94	8.16	13	83.38	8.73	(3, 85)	TRUE	0.113	0.034	TRUE	-0.008	0.255
MPAS - quality of attachment	0			19	41.21	4.33	18	42.06	3.61	19	42.42	3.1	18	42.89	2.17	13	42.77	2.35	(3, 85)	TRUE	0.072	0.018	TRUE	-0.009	0.042
MPAS - absence of hostility	0			19	18.74	3.25	18	19.89	2.78	19	19.21	3.6	18	18.56	3.71	13	19.31	3.95	(3, 85)	TRUE	0.017	0.591	TRUE	0.001	0.827
MPAS - pleasure interaction	0			19	21.37	3.8	18	21.67	3.41	19	21.37	3.93	18	21.5	4.42	13	21.31	4.13	(3, 85)	TRUE	0.021	0.385	TRUE	-0.001	0.878
Estradiol	19	41.63	45.45	19	58.43	85.74	18	39.81	59.44	18	36.32	43.86	18	56.27	109.65	16	37.56	31.8	(3, 106)	TRUE	-0.2	0.788	TRUE	-0.038	0.695
log(Estradiol)	19	3.26	1.03	19	3.32	1.25	18	2.98	1.18	18	3.07	1.06	18	3.16	1.25	16	3.23	1.02	(3, 106)	TRUE	0.002	0.84	TRUE	0.001	0.437
Progesterone	19	0.91	1.47	19	0.12	0.08	18	0.1	0.09	18	1.67	5.61	18	1.25	3.35	16	1.26	3.55	(3, 106)	TRUE	0.039	0.283	TRUE	0	0.987
log(Progesterone)	19	-0.91	1.28	19	-2.36	0.69	18	-2.56	0.62	18	-1.84	1.72	18	-1.96	1.67	16	-1.93	1.67	(3, 106)	TRUE	-0.012	0.495	TRUE	0.005	0.018
Estradiol/Progesterone	19	99.78	100.71	19	512.53	579.35	18	409.66	449.96	18	251.3	235.42	18	422.1	564.39	16	343	308.95	(3, 106)	TRUE	3.174	0.549	FALSE	-1.063	0.121
log(Estradiol/Progesterone)	19	4.17	0.99	19	5.68	1.11	18	5.53	1.01	18	4.91	1.36	18	5.12	1.59	16	5.16	1.49	(3, 106)	TRUE	0.012	0.494	TRUE	-0.004	0.064
Mean FWD	19	0.15	0.06	19	0.16	0.07	18	0.18	0.08	19	0.17	0.08	18	0.16	0.06	17	0.15	0.07	(3, 108)	TRUE	-0.001	0.229	TRUE	0	0.261
Max FWD	19	0.52	0.33	19	0.62	0.29	18	0.74	0.35	19	0.54	0.26	18	0.67	0.43	17	0.51	0.23	(3, 108)	TRUE	-0.002	0.455	TRUE	-0.001	0.056

Extended Data Table 3: Longitudinal sample characteristics.

Data was compared using linear mixed models. Two models were fitted, one ("linear") including only the linear effect of postpartum weeks on the respective variable, followed by a second ("quadratic") that included linear and quadratic effects of time. Abbreviations: LMM = linear mixed model, PP = postpartum, std = standard deviation, df = degrees of freedom, coef = coefficient of investigated LMM effect, EPDS = Edinburgh Postnatal Depression Scale, MPAS = Maternal Postnatal Attachment Scale, FWD = frame-wise displacement.

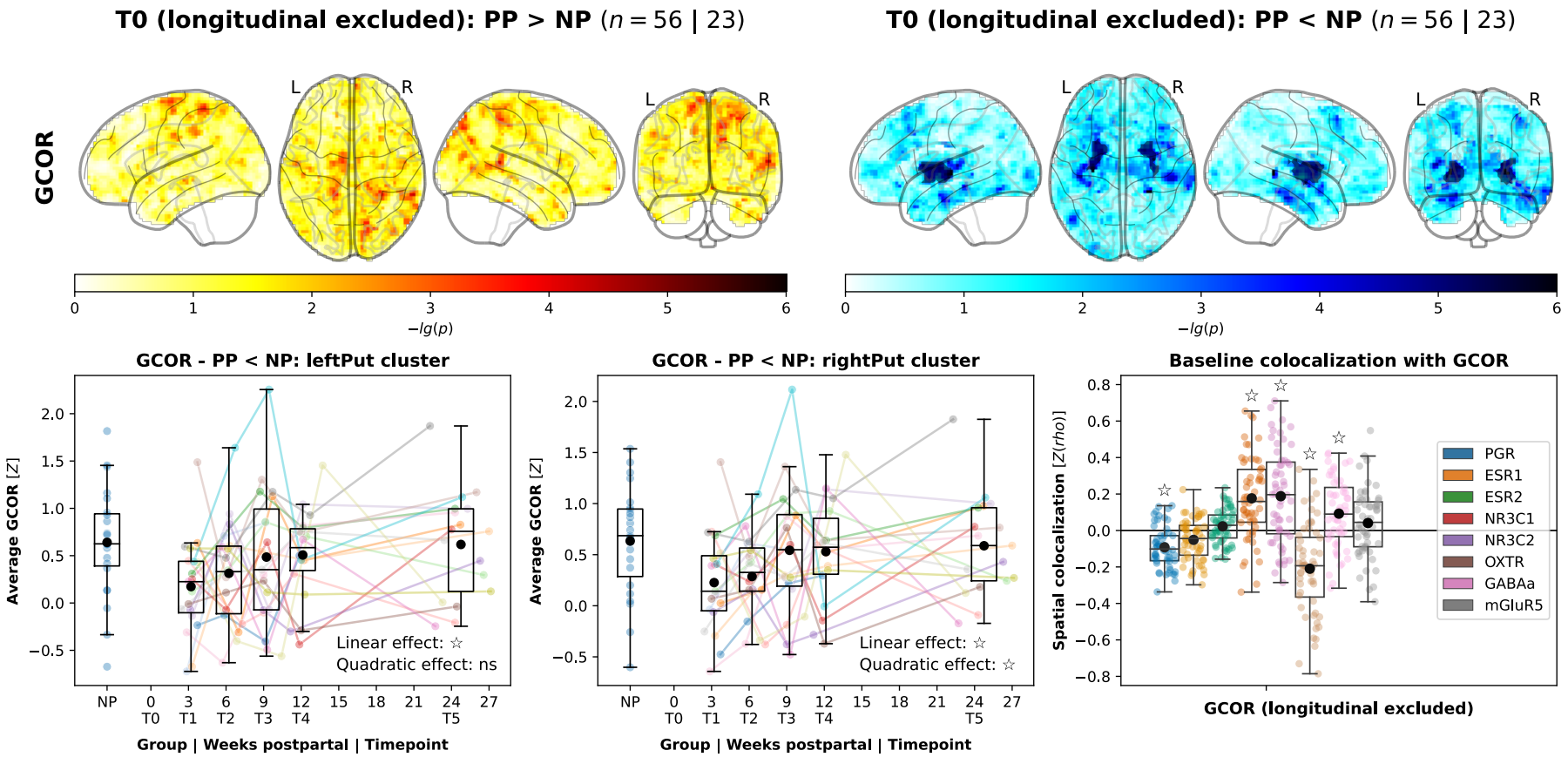

Extended Data Figure 1: GCOR sensitivity analyses to control for regression to the mean effects.

Upper: GCOR whole-brain cluster-level analyses were repeated while excluding subjects with longitudinal data. See Figure 1 for descriptions of plot elements.The resulting clusters almost exactly mirrored the main result. Lower left and center: Longitudinal trajectories of the cluster-average data in the held-out longitudinal sample. See Figure 2 for plot elements. Lower right: Baseline colocalization results without longitudinal subjects. See Figure 3 for plot elements. Temporal trajectories and spatial colocalization results mirrored those from the main analyses. Abbreviations: GCOR = global correlation, PP = postpartum, NP = nulliparous.